Vector theory of four-wave mixing: polarization effects in fiber-optic parametric amplifiers

Qiang Lin and Govind P. Agrawal

Institute of Optics, University of Rochester, Rochester, New York 14627

Received August 4, 2003; revised manuscript received January 29, 2004; accepted February 11, 2004

We present a vector theory of four-wave mixing and use it to study the polarization-dependent nature of four-wave mixing and the conditions under which the gain of a dual-pump fiber-optic parametric amplifier becomes polarization independent. We find that in the absence of self- and cross-phase modulations, any pair of orthogonally polarized pumps can provide polarization-independent gain, but this gain is minimum for linearly polarized pumps and becomes maximum when the two pumps are circularly polarized. Self-and cross-phase modulations induce nonlinear polarization rotation and change the orthogonality between the two pump polarizations. We discuss the general case of elliptically polarized cases and show that only linearly and circularly polarized pumps can maintain their orthogonality along the fiber. A stability analysis shows that the case of linearly polarized pumps is more stable than the circular one against small deviations from the ideal case but that the latter provides much more amplification. © 2004 Optical Society of America

OCIS codes: 060.2320, 060.4370, 190.2620, 190.4380, 190.4970, 260.5430.

1. INTRODUCTION

Fiber-optic parametric amplifiers (FOPAs), based on four-wave mixing (FWM) occurring inside optical fibers, can provide high gain with a relatively flat and wide spectrum when they are pumped in the vicinity of a zero-dispersion wavelength[1–3] or pumped at two well-selected frequencies in this region.[4–7] Recently dual-pump FOPAs have attracted considerable attention because of their potential applications for wideband amplification, wavelength conversion, optical sampling, etc.[1–7] Unfortunately, the parametric gain is strongly polarization dependent because of an intrinsic angular-momentum conservation requirement,[3] and this polarization sensitivity is an obstacle to the practical implementation of FOPAs in optical communication systems. The techniques proposed to solve this problem make use of either polarization diversity[8,9] or linearly orthogonal polarized pumps.[10,11] However, the first technique reduces the gain because half of the pump power propagates in the backward direction inside the diversity loop,[8,9] whereas the nonlinear coupling efficiency is reduced dramatically when the second technique is used.[10,11] In both cases, the amount of FOPA gain or wavelength-conversion efficiency is reduced to relatively small values unless one employs unrealistically high pump powers. It was shown recently that the use of circularly orthogonal polarized pumps can enhance the FWM efficiency.[12]

A natural question one may ask is how does the efficiency of the FWM process in a FOPA depend on the state of polarization (SOP) associated with the two pumps and the signal launched. The existing theory of FWM developed for optical fibers[3] cannot answer this question because it makes the scalar approximation for all electromagnetic fields. What is needed is a full vector theory of the FWM process in optical fibers. In this paper we develop such a vector theory and use it to investigate thoroughly the polarization properties of a FOPA used either for signal amplification or for wavelength conversion. Our theory shows that the nonlinear phenomena of self-phase and cross-phase modulations (SPM and XPM) play an important role in the performance of FOPAs because they can affect the orthogonal nature of the pump SOPs when the pumps are chosen to be orthogonally polarized at the input end. The paper is organized as follows. We first derive in Section 2 the four vector equations governing the FWM process. To gain some physical insight, we first solve them analytically in Section 3 for the special case in which the effects of SPM and XPM are ignored. These nonlinear effects are included in Section 4 to show how the SOP of the two pumps is affected by SPM and XPM. In Section 5 we analyze the general case in which the two pumps and the input signal are elliptically polarized and discuss the conditions under which the FOPA performance can be improved. The main results are summarized in Section 6.

2. VECTOR THEORY OF FOUR-WAVE MIXING

A complete description of dual-pump FOPAs should include all parametric processes originating from degenerate as well as nondegenerate FWM.[4,5] In most experimental situations, the two pumps are located symmetrically 30–40 nm away from the zero-dispersion wavelength of the fiber.[5–7] The resulting gain spectrum exhibits a central flat region in which the dominant contribution comes from a single nondegenerate FWM process corresponding to $\omega_1 + \omega_2 \rightarrow \omega_s + \omega_i$, where ω_1, ω_2, ω_s, and ω_i are the optical frequencies of the two pumps, signal, and idler, respectively. Other FWM processes affect wings of the gain spectrum but leave its flat portion unchanged. Since the flat part is used in practice, we focus only on the above nondegenerate process in the following analysis. Furthermore, we neglect pump deple-

0740-3224/2004/061216-09$15.00

tion because pump powers are much larger than the signal and idler powers in practice. For the same reason, SPM and XPM effects induced by pumps are included, but those induced by signal and idler waves are neglected.

Assuming that the instantaneous electronic response dominates and neglecting the Raman contribution, we find that the third-order nonlinear polarization in a medium such as silica glass is given by[3]

$$\mathbf{P}^{(3)}(\mathbf{r}, t) = \epsilon_0 \vec{\chi}^{(3)} \vdots \mathbf{E}(\mathbf{r}, t)\mathbf{E}(\mathbf{r}, t)\mathbf{E}(\mathbf{r}, t), \tag{1}$$

where $\vec{\chi}^{(3)}$ is the third-order nonlinear susceptibility. If we assume that the nonlinear response is isotropic for silica fibers, the $\vec{\chi}^{(3)}$ has 21 nonzero components,[13] among which only four are independent, which are related to each other as $\chi^{(3)}_{1122} = \chi^{(3)}_{1212} = \chi^{(3)}_{1221} = \chi^{(3)}_{1111}/3$. Thus the third-order nonlinear properties of silica fibers can be expressed in terms of a single parameter $\chi^{(3)}_{1111}$.

In the case of nondegenerate FWM, four distinct optical fields propagate simultaneously inside the optical fiber, and the total electric field satisfying the Maxwell wave equation can be decomposed as

$$\mathbf{E} = \mathrm{Re}[\mathbf{E}_1 \exp(-i\omega_1 t) + \mathbf{E}_2 \exp(-i\omega_2 t) + \mathbf{E}_s \exp(-i\omega_s t) + \mathbf{E}_i \exp(-i\omega_i t)], \tag{2}$$

where Re stands for the real part and $\mathbf{E}_j$ ($j = 1, 2, s, i$) is the slowly varying (complex) amplitudes for the field oscillating at the frequency ω_j. Writing the nonlinear polarization $\mathbf{P}^{(3)}$ also in the same form as

$$\mathbf{P}^{(3)} = \mathrm{Re}[\mathbf{P}_1 \exp(-i\omega_1 t) + \mathbf{P}_2 \exp(-i\omega_2 t) + \mathbf{P}_s \exp(-i\omega_s t) + \mathbf{P}_i \exp(-i\omega_i t)], \tag{3}$$

we find that the slowly varying part at the pump frequencies is given by (ignoring pump depletion)

$$\mathbf{P}_j(\omega_j) = \frac{\epsilon_0 \chi^{(3)}_{111}}{4}[(\mathbf{E}_j \cdot \mathbf{E}_j)\mathbf{E}_j^* + 2(\mathbf{E}_j^* \cdot \mathbf{E}_j)\mathbf{E}_j + 2(\mathbf{E}_m^* \cdot \mathbf{E}_m)\mathbf{E}_j + 2(\mathbf{E}_m \cdot \mathbf{E}_j)\mathbf{E}_m^* + 2(\mathbf{E}_m^* \cdot \mathbf{E}_j)\mathbf{E}_m], \tag{4}$$

where $j, m = 1$ or 2 ($j \neq m$).

By use of the same process, the nonlinear polarization at the signal and idler frequencies is found to be

$$\mathbf{P}_j(\omega_j) = \frac{\epsilon_0 \chi^{(3)}_{1111}}{2}[(\mathbf{E}_1^* \cdot \mathbf{E}_1)\mathbf{E}_j + (\mathbf{E}_1 \cdot \mathbf{E}_j)\mathbf{E}_1^* + (\mathbf{E}_1^* \cdot \mathbf{E}_j)\mathbf{E}_1 + (\mathbf{E}_2^* \cdot \mathbf{E}_2)\mathbf{E}_j + (\mathbf{E}_2 \cdot \mathbf{E}_j)\mathbf{E}_2^* + (\mathbf{E}_2^* \cdot \mathbf{E}_j)\mathbf{E}_2 + (\mathbf{E}_m^* \cdot \mathbf{E}_1)\mathbf{E}_2 + (\mathbf{E}_m^* \cdot \mathbf{E}_2)\mathbf{E}_1 + (\mathbf{E}_1 \cdot \mathbf{E}_2)\mathbf{E}_m^*], \tag{5}$$

where $j, m = s$ or i ($j \neq m$). In Eqs. (4) and (5) the SPM and XPM effects induced by pumps are included, but those induced by signal and idler waves are neglected because of their relatively low power levels.

The four optical fields $\mathbf{E}_j$ ($j = 1, 2, s, i$) evolve along the fiber length according to the Maxwell wave equation. For solving this equation, it is common to choose the z axis along the fiber axis and assume that the vector $\mathbf{E}_j$ lies in the x–y plane. This assumption amounts to neglecting the longitudinal component of the field vectors and is justified in practice as long as the spatial size of the fiber mode is larger than the optical wavelength. To account for the polarization changes, we represent each field as a Jones vector and employ the bra and ket notation of Ref. 14. More specifically, we write the four fields at any point $\mathbf{r}$ inside the fiber as

$$\mathbf{E}_j(\mathbf{r}) = F_j(x, y)|A_j(z)\rangle \exp(i\beta_j z), \tag{6}$$

where $F_j(x, y)$ represents the fiber-mode profile, β_j is the propagation constant at the carrier frequency ω_j, and the Jones vector $|A_j\rangle$ is a two-dimensional column vector representing the two components of the electric field in the x–y plane. The fiber-mode profiles can be taken to be nearly the same for the four fields, $F_j(x, y) \equiv F(x, y)$, which amounts to assuming the same effective core area a_{eff} for the four waves.

Using Eqs. (1)–(6) in the Maxwell wave equation, integrating over the transverse-mode distribution in the x–y plane, and assuming $|A_j\rangle$ to be slowly varying functions of z so that we can neglect its second-order derivative with respect to z, we find that the two pump waves evolve as

$$\frac{\mathrm{d}|A_j\rangle}{\mathrm{d}z} = i\beta_j|A_j\rangle + \frac{i\gamma}{3}(2\langle A_j|A_j\rangle + 2\langle A_m|A_m\rangle + |A_j^*\rangle\langle A_j^*| + 2|A_m\rangle\langle A_m| + 2|A_m^*\rangle\langle A_m^*|)|A_j\rangle, \tag{7}$$

where $j, m = 1$ or 2 ($j \neq m$) and $\langle A|$ and $|A^*\rangle$ are the Hermitian and complex conjugates of $|A\rangle$, respectively. By use of the same procedure, the signal and idler equations are given by

$$\frac{\mathrm{d}|A_j\rangle}{\mathrm{d}z} = i\beta_j|A_j\rangle + \frac{2i\gamma}{3}(\langle A_1|A_1\rangle + \langle A_2|A_2\rangle + |A_1\rangle\langle A_1| + |A_2\rangle\langle A_2| + |A_1^*\rangle\langle A_1^*| + |A_2^*\rangle\langle A_2^*|)|A_j\rangle + \frac{2i\gamma}{3}(\langle A_m|A_1\rangle|A_2\rangle + \langle A_m|A_2\rangle|A_1\rangle + \langle A_1^*|A_2\rangle|A_m^*\rangle), \tag{8}$$

where $j, m = s$ or i ($j \neq m$). Following a similar analysis, it is easy to show that, in the case of a single-pump configuration (degenerate FWM, $2\omega_1 \rightarrow \omega_s + \omega_i$), the signal and idler still follow Eq. (8) if we replace $|A_2\rangle$ with $|A_1\rangle$ and set 2γ to be γ. In this case, the equation for the single-pump field $|A_1\rangle$ is given by Eq. (7) by setting $|A_2\rangle$ to zero.

In these equations, both the SPM and the XPM and the nonlinear phenomenon of FWM are governed by the same nonlinear parameter γ defined as

$$\gamma \equiv n_2 k_0 / a_{\mathrm{eff}} = 3k_0 \chi^{(3)}_{1111}/(8\bar{n} a_{\mathrm{eff}}), \tag{9}$$

where $k_0 = 2\pi/\lambda$ and λ represents an average wavelength for the four waves at which the mode index $\bar{n}$ is specified. The use of a single nonlinear parameter for the four waves is justified because, in practice, the frequency difference among the waves is much smaller than their carrier frequencies. In writing Eqs. (7) and (8), we assume that the fiber is cylindrically symmetric without

birefringence, and fiber losses are neglected because of a short length (<1 km) used typically for making FOPAs. The residual birefringence fluctuations occurring in real optical fibers would affect the FOPA performance, but this topic is beyond the scope of this paper and will be discussed separately.

3. POLARIZATION-DEPENDENT NATURE OF FOUR-WAVE MIXING

In this section we investigate the polarization-dependent nature of FWM inside optical fibers. The vector FWM equations of Section 2 can be used in the general case in which the pumps and the signal are launched into the optical fiber with arbitrary SOPs. However, to investigate the relationship between the FWM efficiency and the pump polarizations as simply as possible, we neglect the SPM and XPM effects temporarily in this section; their impact is considered in Section 4.

Physically, the polarization-dependent nature of FWM inside optical fibers stems from the requirement of angular-momentum conservation among the four interacting photons in an isotropic medium. This requirement can be described most simply in a basis in which $\uparrow$ and $\downarrow$ denote left and right circular polarization states and carry the intrinsic angular momentum (spin) of $+\hbar$ and $-\hbar$, respectively.[15] To describe FWM among arbitrarily polarized optical fields, we decompose each field in this circular polarization basis as $|A_j\rangle = \mathcal{U}_j|\uparrow\rangle + \mathcal{D}_j|\downarrow\rangle$, where $\mathcal{U}_j$ and $\mathcal{D}_j$ represent the field amplitudes in the $\uparrow$ and $\downarrow$ states, respectively, for the jth wave ($j = 1, 2, s, i$). Using this expansion, we can find from Eq. (8) that the creation of idler photons in the two orthogonal spin states is governed by the following two equations (in the absence of XPM):

$$\frac{d\mathcal{U}_i}{dz} = i\beta_i\mathcal{U}_i + \frac{4i\gamma}{3}[\mathcal{U}_1\mathcal{U}_2\mathcal{U}_s^* + (\mathcal{U}_1\mathcal{D}_2 + \mathcal{D}_1\mathcal{U}_2)\mathcal{D}_s^*], \tag{10}$$

$$\frac{d\mathcal{D}_i}{dz} = i\beta_i\mathcal{D}_i + \frac{4i\gamma}{3}[\mathcal{D}_1\mathcal{D}_2\mathcal{D}_s^* + (\mathcal{U}_1\mathcal{D}_2 + \mathcal{D}_1\mathcal{U}_2)\mathcal{U}_s^*]. \tag{11}$$

The same equations hold for the signal if we exchange the subscript s and i.

The three terms on the right side of Eqs. (10) and (11) show clearly the different angular-momentum combinations of the interacting photons and lead to the following selection rules for the FWM process. The first term $\mathcal{U}_1\mathcal{U}_2\mathcal{U}_s^*$ in Eq. (10) corresponds to the path $\uparrow_1 + \uparrow_2 \rightarrow \uparrow_s + \uparrow_i$, whereas the first term $\mathcal{D}_1\mathcal{D}_2\mathcal{D}_s^*$ in Eq. (11) corresponds to the path $\downarrow_1 + \downarrow_2 \rightarrow \downarrow_s + \downarrow_i$, where a subscript denote photons at that specific frequency. Physically, if both pump photons are in the $\uparrow$ or $\downarrow$ state with a total angular momentum of $\pm 2\hbar$, the signal and idler photons must also be in the same state to conserve the total angular momentum.

The last two terms in Eq. (10) correspond to the paths $\uparrow_1 + \downarrow_2 \rightarrow \downarrow_s + \uparrow_i$ and $\downarrow_1 + \uparrow_2 \rightarrow \downarrow_s + \uparrow_i$. The only difference for the last two terms in Eq. (11) is that the same two combinations of pump photons produce a signal–idler pair as $\uparrow_s + \downarrow_i$. The main point to note is that these four terms use orthogonally polarized pump photons with zero net angular momentum and thus must produce orthogonally polarized signal and idler photons in the basis used. A signal photon with state $\uparrow_s$ can couple only to an idler photon with state $\downarrow_i$ and vice versa. This leads to two possible combinations, $\uparrow_s + \downarrow_i$ and $\downarrow_s + \uparrow_i$, both of which are equally probable.

A pump with an arbitrary polarization is composed of photons in both the $\uparrow$ and the $\downarrow$ states with different amplitudes and phases. FWM in this case includes both scenarios discussed above. Its polarization dependence is a consequence of the fact that different paths occur with different probabilities and couple with each other, and one must add probability amplitudes to sum over various paths (as is done in quantum mechanics). The coupling of different paths and the addition of amplitudes can lead to constructive or destructive interference. For example, if the two pumps are right circularly polarized, no FWM can occur for a signal that is left circularly polarized (and vice versa). The same selection rules hold for degenerate FWM, since the same set of equations, Eqs. (10) and (11), applies after we replace $|A_2\rangle$ with $|A_1\rangle$ and 2γ with γ. It follows immediately that the output of any single-pump FOPA is always polarization dependent because the two pump photons have the same SOP. More importantly, it is impossible to balance the FWM efficiency experienced by the $\uparrow$ and $\downarrow$ components of the signal unless a polarization diversity loop is used.

In the case of lightwave system applications, one is interested in the FOPA configuration that would yield the same signal gain irrespective of the SOP of the input signal (polarization-independent gain). A detailed analysis of Eqs. (10) and (11) shows that this can be realized by two pumps with orthogonal polarizations, no matter what their individual SOPs are. Although an elliptically polarized pump consists of a mixture of $\uparrow$ and $\downarrow$ states, it turns out that, for two pumps with orthogonal elliptical polarizations, the two paths, $\uparrow_1 + \uparrow_2 \rightarrow \uparrow_s + \uparrow_i$ and $\downarrow_1 + \downarrow_2 \rightarrow \downarrow_s + \downarrow_i$, not only have the same efficiency but also have appropriate relative phases with the polarization-independent paths ($\uparrow_1 + \downarrow_2$ or $\downarrow_1 + \uparrow_2$) $\rightarrow$ ($\downarrow_s + \uparrow_i$ or $\uparrow_s + \downarrow_i$). As a result, elliptically but orthogonally polarized pumps can provide a polarization-independent FWM. More specifically, if the two pumps are orthogonally and circularly polarized, the terms containing $\mathcal{U}_1\mathcal{U}_2$ and $\mathcal{D}_1\mathcal{D}_2$, vanish, and the FWM process becomes polarization independent. If the two pumps are orthogonally but linearly polarized, it turns out that $\mathcal{U}_1\mathcal{D}_2 + \mathcal{D}_1\mathcal{U}_2 = 0$. The possible paths in this case, ($\uparrow_1 + \downarrow_2$) $\rightarrow$ ($\downarrow_s + \uparrow_i$ or $\uparrow_s + \downarrow_i$) and ($\downarrow_1 + \uparrow_2$) $\rightarrow$ ($\downarrow_s + \uparrow_i$ or $\uparrow_s + \downarrow_i$), are out of phase with each other and thus cancel. The remaining two paths, $\uparrow_1 + \uparrow_2 \rightarrow \uparrow_s + \uparrow_i$ and $\downarrow_1 + \downarrow_2 \rightarrow \downarrow_s + \downarrow_i$, have the same efficiency. In the following analysis, we focus on such polarization-independent FWM but employ a basis of linear polarization because this basis provides a more convenient way to discuss the polarization ellipticity of pumps.[16]

By noting that Eqs. (7) and (8) are invariant with respect to rotations in the x–y plane, we choose x and y axes along the principal axes of the ellipse of the pump polarization without any loss of generality. Solving Eq. (7) with $\gamma = 0$, it is easy to see that the Jones vectors of the

two elliptically but orthogonally polarized pumps then evolve as

$$|A_1(z)\rangle = \sqrt{P_1}\begin{pmatrix}\cos\theta\\ i\sin\theta\end{pmatrix}\exp(i\beta_1 z),$$
$$|A_2(z)\rangle = \sqrt{P_2}\begin{pmatrix}i\sin\theta\\ \cos\theta\end{pmatrix}\exp(i\beta_2 z), \quad (12)$$

where P_1 and P_2 are the input powers of two pumps and θ is the angle characterizing the ellipticity. This equation shows that the pump SOP does not change in the absence of SPM and XPM effects and the two pumps remain orthogonally polarized inside the fiber.

Using Eq. (12) in Eq. (8) and introducing $|A_s\rangle = |B_s\rangle\exp(i\beta_s z)$ and $|A_i\rangle = |B_i\rangle\exp(i\beta_i z)$, we find that the signal and idler fields evolve as

$$\frac{d|B_s\rangle}{dz} = \frac{2i\gamma}{3}\sqrt{P_1P_2}\exp(-i\Delta\beta z)(2i\sin 2\theta\sigma_0 + \cos 2\theta\sigma_2)|B_i^*\rangle, \quad (13)$$

$$\frac{d|B_i\rangle}{dz} = \frac{2i\gamma}{3}\sqrt{P_1P_2}\exp(-i\Delta\beta z)(2i\sin 2\theta\sigma_0 + \cos 2\theta\sigma_2)|B_s^*\rangle, \quad (14)$$

where $\Delta\beta = \beta_s + \beta_i - \beta_1 - \beta_2$ represents the linear phase mismatch, σ_0 is a unit matrix, and the Pauli matrices are introduced as[3]

$$\sigma_1 = \begin{bmatrix}1 & 0\\ 0 & -1\end{bmatrix}, \qquad \sigma_2 = \begin{bmatrix}0 & 1\\ 1 & 0\end{bmatrix}, \qquad \sigma_3 = \begin{bmatrix}0 & -i\\ i & 0\end{bmatrix}. \quad (15)$$

These equations show that the parametric gain depends on the pump ellipticity θ.

Equations (13) and (14) are easy to solve and provide the following solution for the signal field:

$$|B_s(z)\rangle = |B_s(0)\rangle \times\left[\cosh(gz) + \frac{i\Delta\beta}{2g}\sinh(gz)\right]\exp(-i\Delta\beta z/2), \quad (16)$$

where the parametric gain is given by

$$g(\theta) = [(2\gamma/3)^2 P_1P_2(1 + 3\sin^2 2\theta) - (\Delta\beta/2)^2]^{1/2}. \quad (17)$$

Since the signal is amplified by the same factor for any SOP, it is clear that, in the absence of SPM and XPM, the nondegenerate FWM process is polarization independent for any two orthogonally polarized pumps. However, the overall FWM efficiency depends on the exact state of pump polarizations through the θ dependence of the parametric gain.

Figure 1 shows the θ dependence of g after one's normalizing it by $\eta = 4\gamma\sqrt{P_1P_2}/3$ for two values of linear phase mismatch. The parametric gain is maximum for $\theta = 45°$, which corresponds to circularly polarized pumps but becomes minimum when $\theta = 0°$, which corresponds to linearly polarized pumps. This can be understood simply from Eq. (8) directly. In fact, the first two terms among the last three FWM terms in Eq. (8) are the same

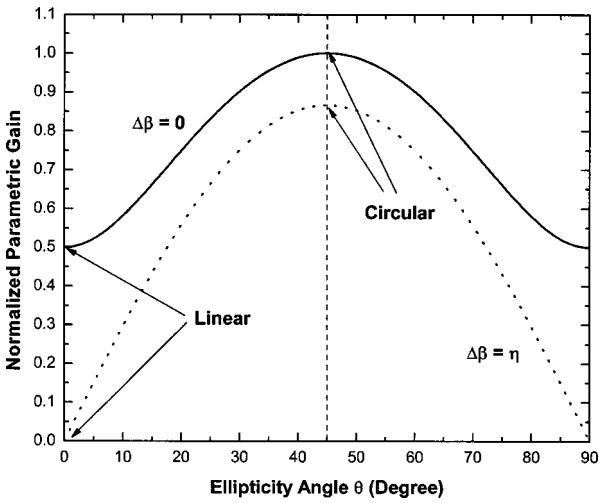

Fig. 1. Normalized parametric gain as a function of pump ellipticity angle. The two pumps are assumed to be orthogonally polarized. The solid curve shows the case in which the phase-matching condition is perfectly satisfied. The dotted curve shows the case of a finite phase mismatch for $\Delta\beta = \eta = 4\gamma\sqrt{P_1P_2}/3$.

for any pair of orthogonally polarized pumps. The overall FWM efficiency is thus dictated by the last term. Noting that $|A^*\rangle$ has the same ellipticity as $|A\rangle$ but opposite handedness, one can see that the inner product $|\langle A_{p1}^*|A_{p2}\rangle|$ for two orthogonally polarized pumps is maximum when the two pumps are circularly polarized but is zero when the two pumps are linearly polarized.

4. PUMP POLARIZATION EVOLUTION

We now consider the general case and allow for the SPM and XPM effects induced by the two pumps. The situation changes considerably in the presence of SPM and XPM, both of which can change the SOP of an optical field if they produce nonlinear phase shifts that are different for the two components of the Jones vector. Any such differential phase shift changes the SOP through a phenomenon known as nonlinear polarization rotation (NPR).

To see how the SOP of the two pumps changes owing to NPR, it is useful to write Eq. (7) in the Stokes space after introducing the Stokes vectors of the two pumps as

$$\vec{S}_{p1} = \langle A_1|\vec{\sigma}|A_1\rangle, \qquad \vec{S}_{p2} = \langle A_2|\vec{\sigma}|A_2\rangle, \quad (18)$$

where $\vec{\sigma} = \sigma_1\hat{e}_1 + \sigma_2\hat{e}_2 + \sigma_3\hat{e}_3$. Here $\hat{e}_j$ $(j = 1, 2, 3)$ are the three unit vectors in the Stokes space, respectively. Since the magnitude of the Stokes vectors $\vec{S}_{p1}$ and $\vec{S}_{p2}$ represents pump powers that do not change (in the absence of losses and pump depletion), the Stokes vectors move on the surface of a sphere, known as the Poincaré sphere. The Stokes vector lies in the equatorial plane for linearly polarized light and points toward the north and south poles for circularly polarized light. According to the convention used for Eqs. (12), the directions $\hat{e}_1$ and $\hat{e}_3$ correspond to the linear and left circular polarization, respectively. Orthogonally polarized pumps are represented by two Stokes vectors that are antiparallel; i.e., they point in the opposite directions on the Poincaré sphere.

It is easy to show from Eq. (7) that the Stokes vectors $\vec{S}_{p1}$ and $\vec{S}_{p2}$ satisfy

$$\frac{d\vec{S}_{p1}}{dz} = \frac{2\gamma}{3}[(\vec{S}_{p1} + 2\vec{S}_{p2})_3\hat{e}_3 - 2\vec{S}_{p2}] \times \vec{S}_{p1}, \quad (19)$$

$$\frac{d\vec{S}_{p2}}{dz} = \frac{2\gamma}{3}[(\vec{S}_{p2} + 2\vec{S}_{p1})_3\hat{e}_3 - 2\vec{S}_{p1}] \times \vec{S}_{p2}, \quad (20)$$

where the subscript 3 denotes the component along the vertical $\hat{e}_3$ direction. These equations show that the SPM rotates the Stokes vector along the vertical direction. In contrast, the two XPM terms combine such that the XPM rotates the Stokes vector along a vector that lies in the equatorial plane.

Now consider how the two pumps rotate the Stokes vector of the signal and idler waves. The signal is assumed to be weak enough that the SPM-induced NPR can be neglected. However, the two pumps will change its SOP through XPM. If the two pumps have the same power and are orthogonally polarized, it turns out that the signal and idler polarizations remain unaffected. Physically speaking, even though each pump will change the signal SOP, their orthogonality and the antiparallel Stokes vectors cancel the individual rotations. Thus we conclude that the SOPs of the signal and idler will not change if the pumps with an equal power were to maintain their orthogonal nature during propagation. However, the two pumps cannot maintain their orthogonality because the SPM- and XPM-induced NPR cannot be neglected for them.

We have solved Eqs. (19) and (20) numerically to study how the pump SOP changes with propagation inside the fiber. On the Poincaré sphere, an arbitrary SOP is characterized by the latitude angle ψ and azimuthal angle φ associated with the spherical coordinates. The connection between the ellipticity angle θ and the spherical coordinate ψ is provided by the well-known relation $\psi = 2\theta$.[16] We use θ as an input parameter to present our numerical results. As a rotation in the x–y plane in the Jones space corresponds to a rotation around $\hat{e}_3$ in the Stokes space, and Eq. (7) is invariant to such a rotation, the azimuthal angle φ does not play an important role in this analysis.

Figure 2 shows the trajectories of $\vec{S}_{p1}$ on the Poincaré sphere for four different input values $\theta = 2°$, 15°, 30°, and 43°. The vector $\vec{S}_{p2}$ is set to be antiparallel to $\vec{S}_{p1}$ at the input end to ensure the initial pump orthogonality. The combined effect of SPM and XPM causes the pump polarization to rotate around the $\hat{e}_1$ axis. However, the two pumps can maintain their orthogonality when both of them are either circularly polarized or linearly polarized because these two SOPs represent the fixed points of Eqs. (19) and (20). We thus conclude that a dual-pump FOPA can be polarization independent only when the two pumps are linearly or circularly polarized while being orthogonal at the input end of the fiber.

Which of the two pumping configurations is desirable in practice? An important question that must be answered is related to the stability of the two fixed points, which must be stable against small perturbations over the entire fiber length for the pumping configuration to be useful. To answer this question, one can perform a linear stability analysis of the two fixed points occurring for $\theta = 0°$ and 45° or study numerically how the SOP of the two pumps changes when θ deviates slightly from these values. The numerical results of Fig. 2 show how the SOP of one of the pumps evolves on the Poincaré sphere for several values of θ. The $\theta = 0°$ fixed point on the $\hat{e}_1$ axis is stable because the Stokes vector remains confined to its vicinity even when $\theta = 2°$. In contrast, the fixed point at the $\hat{e}_3$ axis occurring for $\theta = 45°$ is not stable, since the Stokes vector deviates far from it for $\theta = 43°$ if the fiber is long enough.[17,18]

In practice, FOPAs are typically designed by use of high-nonlinearity fiber ($\gamma \sim 10\ \mathrm{W}^{-1}/\mathrm{km}$) so that one needs short fiber lengths ~1 km or less.[5] It is thus possible that the instability of the circularly polarized pump will not affect the FWM process significantly over the FOPA length. The length scale over which pump polarization evolves is set by the nonlinear length defined as $L_N = 3/(2\gamma\sqrt{P_1P_2})$. As an example, in the case of two pumps with powers of 0.5 W, each propagating along a 500-m-long high-nonlinearity fiber with $\gamma = 10\ \mathrm{W}^{-1}/\mathrm{km}$, the fiber length L corresponds to $L = 1.7L_N$. Figure 3(a) shows how the pump SOP evolves for such a FOPA for the same four angles used in Fig. 2. The tip of each curve corresponds to $z = L$. As seen there, the $\theta = 43°$ curve does not deviate too far from the $\theta = 45°$ location. In practice, deviations will be even smaller as one approaches $\theta = 45°$. Thus circularly polarized pumps can be used for such a short-length FOPA because a small perturbation from the circular polarization does not lead to too much deviation from the ideal $\theta = 45°$ case.

The impact of SPM and XPM on the FWM process can also be studied by considering the inner product defined as $\rho = (\vec{S}_{p1} \cdot \vec{S}_{p2})/(P_1P_2)$. When $\rho = -1$, the two Stokes vectors are antiparallel and the two pumps SOPS are orthogonal to each other. For $\theta = 0°$ and $\theta = 45°$, $\rho = -1$ initially and remains -1 at all points along the fiber. Figure 3(b) shows how this quantity varies along

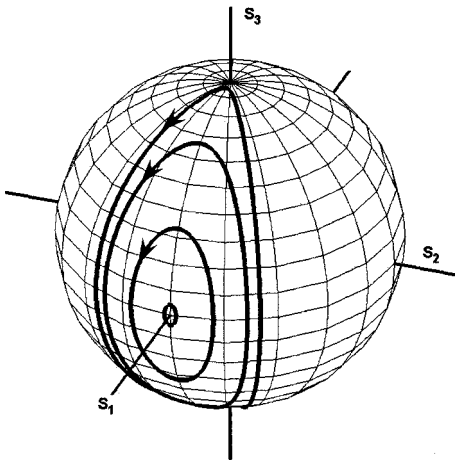

Fig. 2. Evolution of the SOP of one of the pumps on the Poincaré sphere over a long propagation distance. The two pumps are orthogonal initially. The four trajectories correspond to a pump ellipticity angle $\theta = 2°$, 15°, 30°, and 43°, beginning from the inside.

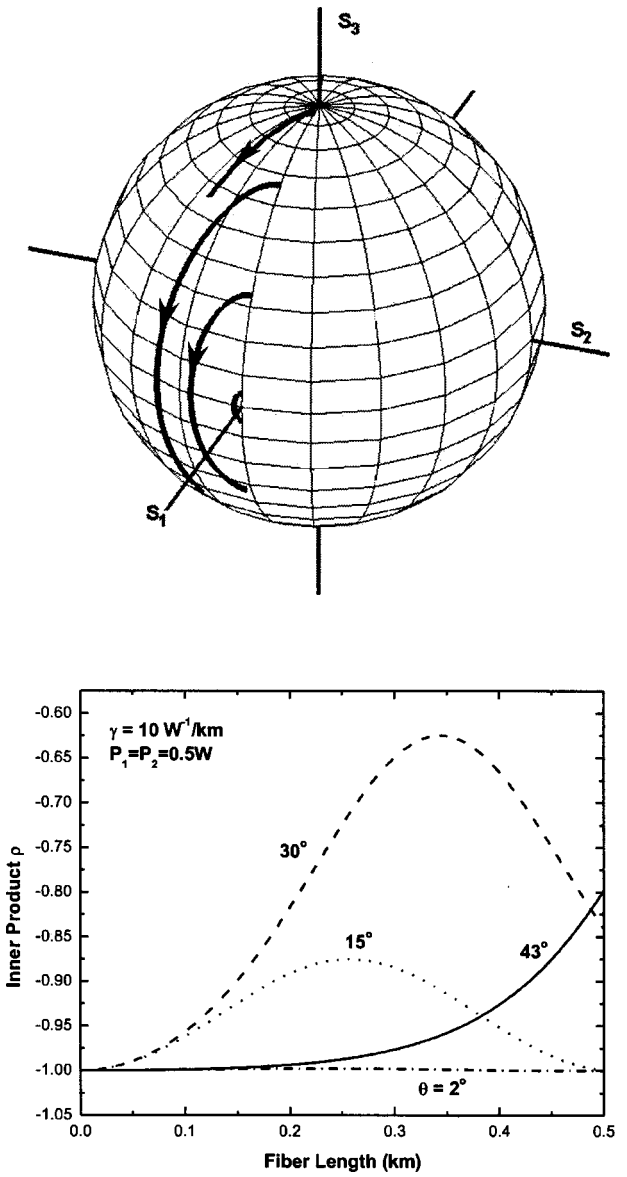

Fig. 3. (a) Pump SOP evolution for the same four values of θ for a 500-m-long fiber with $\gamma = 10\ \mathrm{W}^{-1}/\mathrm{km}$. The two pumps have equal powers of 0.5 W. (b) The inner product ρ as a function of propagation distance for the same fiber. Pumps are orthogonally polarized when $\rho = -1$.

the fiber length for the four values of θ whose trajectories are shown on the Poincaré sphere. When the pump SOPs deviate from being linear by $\theta = 2°$, the orthogonality is nearly maintained over the whole fiber. When $\theta = 15°$, the pumps begin to deviate from being orthogonal within 100 m of fiber. Deviations become much larger in the case of $\theta = 30°$. But for $\theta = 43°$, ρ evolves slowly and begins to deviate from its initial value of -1 only after $L > L_N$. As a result, this configuration provides much higher gain while keeping the polarization-dependent gain (PDG) relatively small as long as $L \leq L_N$.

5. POLARIZATION-DEPENDENT GAIN

Having shown that both the linear and the circular polarization states for the two orthogonally polarized pumps can provide polarization-independent gain, we compare in this section the relative performance of such FOPAs. Although a general solution of Eq. (8) requires a numerical approach, the vector problem reduces to a scalar problem whenever the pumps maintain their SOPs along the fiber because Eq. (8) can be easily diagonalized. It provides the following expression for the FOPA gain[3]:

$$G \equiv \frac{\langle A_s(L)|A_s(L)\rangle}{\langle A_s(0)|A_s(0)\rangle} = 1 + [1 + \kappa^2/(4g^2)]\sinh^2(gL), \tag{21}$$

where $\kappa = \Delta\beta + r_\kappa\gamma(P_1 + P_2)$ is the total phase mismatch among the four waves (it includes the contributions of both the fiber dispersion and the pump-induced XPM and SPM) and $g = [(r_g\gamma)^2 P_1 P_2 - (\kappa/2)^2]^{1/2}$ is the parametric gain coefficient. In the expressions of κ and g, r_κ and r_g are quantities that depend on the polarizations of the pumps and signal. $r_\kappa = 1$ and $r_g = 2/3$ when the two pumps are orthogonally and linearly polarized, but $r_\kappa = 2/3$ and $r_g = 4/3$ when the two pumps are orthogonally but circularly polarized. The doubling of r_g in the latter case implies a significant improvement in the amount of FOPA gain. Actually, the same values of r_κ and r_g ($r_\kappa = 2/3$ and $r_g = 4/3$) hold if the signal is copolarized with the two circularly copolarized pumps. In contrast, when both pumps and the signal are linearly copolarized, $r_\kappa = 1$ and $r_g = 2$.[3] Although r_g is maximum in this case and the FOPA provides maximum gain, it is also highly polarization dependent. This can be seen by noting that $r_\kappa = -5/3$ and $r_g = 2/3$ when the signal is orthogonally polarized with respect to the two linearly copolarized pumps. The difference in r_κ and r_g for different pumping configurations affect the phase matching and FWM efficiency considerably and provide different FOPA performances. We discuss such differences in detail in the following analysis.

Figure 4 shows the gain spectra for three different

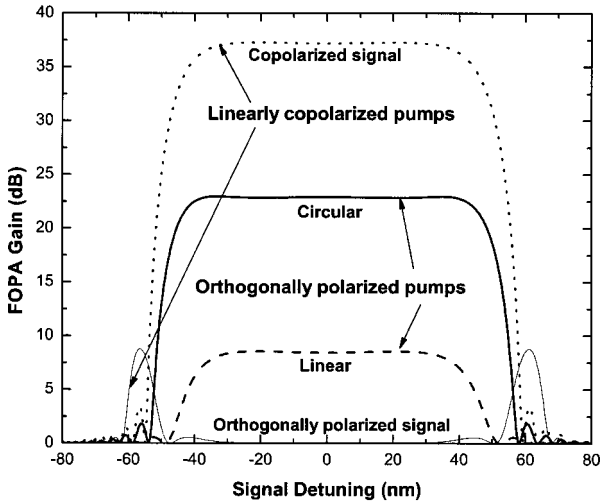

Fig. 4. Gain as a function of signal detuning from the zero-dispersion wavelength ($\lambda_0 = 1580$ nm) for a 500-m-long FOPA pumped by use of two 0.5-W pumps located at 1535 and 1628 nm. Pumps are orthogonally polarized for the middle two curves for which gain does not depend on the state of signal polarization. The thin solid and dotted curves show the dependence of gain on signal polarization in the case of linearly copolarized pumps.

pumping schemes that use $\gamma = 10\ \mathrm{W}^{-1}/\mathrm{km}$, $\lambda_0 = 1580\ \mathrm{nm}$, $\beta_3 = 0.04\ \mathrm{ps}^3/\mathrm{km}$, $\beta_4 = 1.0 \times 10^{-4}\ \mathrm{ps}^4/\mathrm{km}$, and $L = 500\ \mathrm{m}$. The two pump wavelengths ($\lambda_1 = 1535\ \mathrm{nm}$ and $\lambda_2 = 1628\ \mathrm{nm}$) and their powers ($P_1 = P_2 = 0.5\ \mathrm{W}$) are chosen such that the FOPA provides a fairly flat gain of 37 dB over a wide wavelength range (dotted curve) when the two pumps as well as the signal are linearly copolarized. As discussed earlier, this gain is highly polarization dependent. When the signal becomes orthogonally polarized to the two copolarized pumps, the FOPA gain is reduced to almost zero in the central part (thin solid curve) because of large variations in the FWM efficiency and XPM-induced phase mismatch. When two orthogonal linearly polarized pumps are used, the gain spectrum is still wide and flat (dashed curve), but the gain is reduced dramatically to a quite small value of around 8.5 dB. However, as shown by the solid curve, the FOPA gain can be increased from 8.5 to 23 dB over a wider spectral region if the two pumps are made left and right circularly polarized. Thus circular polarization is superior to linear polarization because it provides more gain at a given pump power. Alternatively, it can provide the same gain with only half the pump power as seen from Fig. 1 and also found in Ref. 12.

To see how much PDG is induced when one deviates from the ideal values of $\theta = 0°$ and $\theta = 45°$, one can see in Fig. 5 the FOPA gain for the same four values of θ used in Fig. 3. In all cases, two pump polarizations are orthogonal at the input end. The gain spectra in the nonideal cases are obtained by solving Eqs. (7) and (8) numerically. The solid curves in Fig. 5(a) show the case in which the signal is linearly polarized at 45° at the input end (the polarization angle is in the Jones space, corresponding to its Stokes vector along the $\hat{e}_2$ axis in the Stokes space). The solid curves in Fig. 5(b) show cases in which the signal is linearly polarized at 135° at the input end (Stokes vector along the negative $\hat{e}_2$ axis). These two signal polarizations correspond to the minimum and maximum FOPA gain and thus provide the magnitude of PDG. In all cases, the flatness of the gain spectra is maintained to a good extent because of the dual-pump nature of the FOPA. The two dotted curves show the linear ($\theta = 0°$) and circular ($\theta = 45°$) polarization cases for which the gain is polarization independent. A small perturbation of $\theta = 2°$ from the linear polarization produces a PDG of 1.3 dB in the central part of the gain spectrum. This PDG increases with the ellipticity of the pump polarization and can reach 14.7 dB when $\theta = 30°$. It decreases when the pump SOP tends toward circular polarization. As shown by the 43° curves, a perturbation of 2° from the ideal circular polarization produces a PDG of 3.4 dB. Although this amount is larger than that for linear polarization, the overall FOPA gain is much larger that that for linear orthogonal polarization. The spectrum is also wider and flatter.

To show how the signal SOP affects the FOPA gain, we assume that the signal is linearly polarized and vary the polarization angle ϕ (in the range 0 to π in the Jones space). Figure 6(a) shows how the gain varies with ϕ for a 1590-nm signal located in the central part of the gain spectrum for several different pump polarizations. When the two pumps are linearly copolarized, the gain is highly

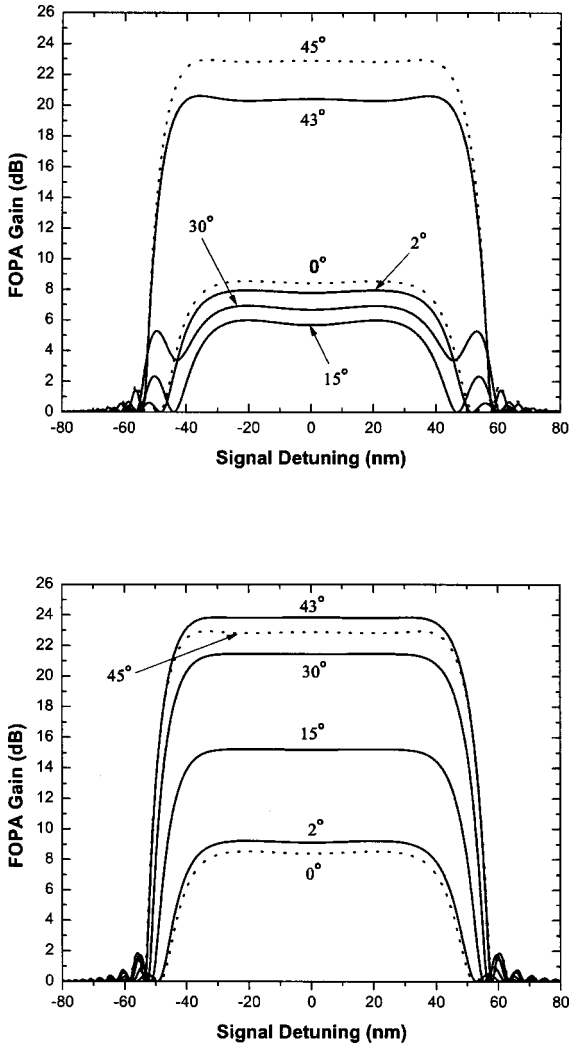

Fig. 5. Gain as a function of signal detuning from the zero-dispersion wavelength under different pump polarizations. Other parameters are the same as Fig. 4(a) Solid curves show the cases in which the signal is linearly polarized ($\phi = 45°$) such that it experiences minimum gain. (b) Solid curves show the cases in which the signal is linearly polarized ($\phi = 135°$) such that it experiences maximum gain. The two dotted curves show the cases in which the two pumps are linearly or circularly polarized.

polarization dependent and can vary from a maximum value of around 37 dB to a minimum value of 0, depending on the signal SOP (dotted curve). This polarization sensitivity can be overcome by use of pumps with orthogonal linear polarizations ($\theta = 0$). However, such a scheme can provide only a small amount of gain (lower dashed line). The situation changes if the two pumps are orthogonal circularly polarized ($\theta = 45°$). This scheme not only maintains a high value of flat gain but the FOPA gain is also completely invariant with signal polarization (upper dashed curve). Small changes in θ from these ideal values produce some PDG as seen by the curves for $\theta = 2°$ and 43°.

When the pumps become elliptically polarized, the FOPA gain is considerably polarization dependent. The gain extrema occur when the signal polarization angle is 45° and 135°, where the Stokes vector is perpendicular to

those of the pumps. Although the linear polarization of the signal is considered here, it turns out that these two signal SOPs correspond to the two global extrema of the FOPA gain. The FOPA gain at $\phi = 135°$ is larger than that at $\phi = 45°$ because of the nature of pump polarization evolution shown in Fig. 3(a). Both pumps evolve such that their Stokes vectors are closer to that of the signal for $\phi = 135°$ and thus provide more gain. Figure 6(b) shows the dependence of minimum and maximum FOPA gain and the corresponding PDG (dotted curve) on the pump ellipticity angle θ. It can be seen clearly that PDG is zero when the two pumps are linearly or circularly polarized while remaining orthogonal. When the two pumps are elliptically polarized at the input end, the PDG can be as large as 14.7 dB for $\theta = 30°$ because of SPM- and XPM-induced polarization changes.

Although we have focused on the phenomenon of signal amplification, our results also apply to FWM-based wavelength converters with only minor changes. Since the signal and idler photons are created simultaneously, the idler power $P_i = \langle A_i|A_i\rangle$ is related to the signal power P_s as $P_i(L) = P_s(L) - P_s(0)$ if we neglect a relatively small difference between the signal and the idler photon energies. The wavelength-conversion efficiency η is thus related to the signal gain $G = P_s(L)/P_s(0)$ as $\eta \equiv P_i(L)/P_s(0) = G - 1$. As a result, the entire discussion related to signal amplification applies to wavelength conversion.

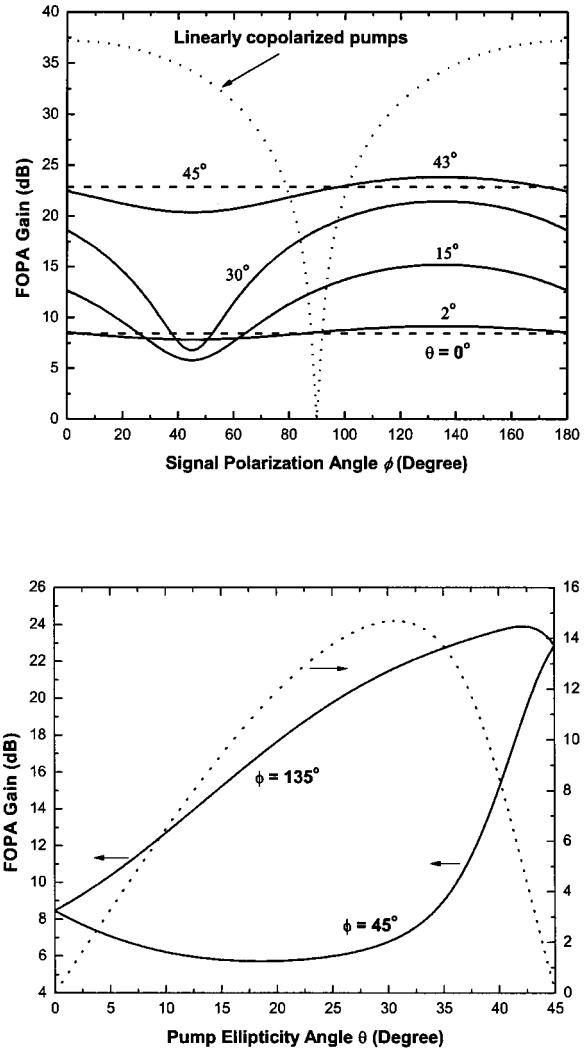

Fig. 6. (a) Gain as a function of signal polarization angle ϕ for the same FOPA under different pumping configurations. (b) The maximum and minimum gains (solid curves) and the amount of PDG (dotted curve) as a function of pump ellipticity angle for the FOPA of Fig. 4.

6. SUMMARY

We have developed a general vector theory of the nonlinear FWM process and have used it to study the impact of pump polarization configuration on the performance of FOPAs. We show that orthogonally but linearly polarized pumps provide polarization-independent gain but reduce its magnitude drastically compared with the case of linearly copolarized pumps and signal. In the absence of SPM and XPM, any orthogonally polarized pumps can provide a polarization-independent FOPA gain. However, the gain is minimum for linear polarization and becomes maximum when the two pumps are orthogonal circularly polarized. SPM- and XPM-induced polarization changes destroy the orthogonality between the two pumps and induce PDG for all elliptically and orthogonally polarized pumps except when the ellipticity angle $\theta = 0$ or 45°. These two configurations provide completely polarization-independent parametric amplification and have similar resistance to small polarization perturbations for fibers whose length is comparable with or shorter than the nonlinear length, although circular polarization performs worse for longer fibers. We show that the FOPA gain or the wavelength-conversion efficiency can be enhanced by a factor of 25 or more by changing the linear polarization to circular polarization while maintaining the orthogonality between the two pumps.

The theoretical analysis in this paper is based on the assumption that the fiber used for making a FOPA has no birefringence. If the fiber has high polarization-mode dispersion, random variations in the states of polarization of the four waves eventually eliminate the distinction between linear and circular polarizations. As a result, any orthogonally polarized pumping configuration will have nearly the same performance. Moreover, the frequency-dependent birefringence will change the relative polarization orientations among the four waves depending on their wavelength separation and thus would make the PDG frequency dependent. The vector theory presented here can be extended to investigate the polarization-mode-dispersion effects on FOPA performance. A detailed analysis is beyond the scope of this paper and will be discussed elsewhere.[19,20]

ACKNOWLEDGMENTS

The authors thank S. Radic and C. J. McKinstrie for helpful discussions. This research is partially supported by the National Science Foundation under grants ECS-0320816 and ECS-0334982.

Q. Lin, the corresponding author, can be reached by e-mail at linq@optics.rochester.edu.

REFERENCES

1. J. Hansryd, P. A. Andrekson, M. Westlund, J. Li, and P. O. Hedekvist, "Fiber-based optical parametric amplifiers and their applications," IEEE J. Sel. Top. Quantum Electron. **8**, 506–520 (2002).
2. M. N. Islam and Ö. Boyraz, "Fiber parametric amplifiers for wavelength band conversion," IEEE J. Sel. Top. Quantum Electron. **8**, 527–537 (2002).
3. G. P. Agrawal, *Nonlinear Fiber Optics*, 3rd ed. (Academic, San Diego, Calif. 2001).
4. C. J. McKinstrie, S. Radic, and A. R. Chraplyvy, "Parametric amplifiers driven by two pump waves," IEEE J. Sel. Top. Quantum Electron. **8**, 538–547 (2002).
5. S. Radic, C. J. McKinstrie, A. R. Chraplyvy, G. Raybon, J. C. Centanni, C. G. Jorgensen, K. Brar, and C. Headley, "Continuous-wave parametric gain synthesis using nondegenerate pump four-wave mixing," IEEE Photon. Technol. Lett. **14**, 1406–1408 (2002).
6. S. Radic and C. J. McKinstrie, "Two-pump fiber parametric amplifiers," Opt. Fiber Technol. **9**, 7–23 (2003).
7. S. Radic, C. J. McKinstrie, R. M. Jopson, J. C. Centanni, Q. Lin, and G. P. Agrawal, "Record performance of parametric amplifier constructed with highly nonlinear fiber," Electron. Lett. **39**, 838–840 (2003).
8. T. Hasegawa, K. Inoue, and K. Oda, "Polarization independent frequency conversion by fiber four-wave mixing with a polarization diversity technique," IEEE Photon. Technol. Lett. **5**, 947–949 (1993).
9. K. K. Y. Wong, M. E. Marhic, K. Uesaka, and L. G. Kazovsky, "Polarization-independent one-pump fiber-optical parametric amplifier," IEEE Photon. Technol. Lett. **14**, 1506–1508 (2002).
10. K. Inoue, "Polarization independent wavelength conversion using fiber four-wave mixing with two orthogonal pump lights of different frequencies," J. Lightwave Technol. **12**, 1916–1920 (1994).
11. K. K. Y. Wong, M. E. Marhic, K. Uesaka, and L. G. Kazovsky, "Polarization-independent two-pump fiber optical parametric amplifier," IEEE Photon. Technol. Lett. **14**, 911–913 (2002).
12. M. E. Marhic, K. K. Y. Wong, and L. G. Kazovsky, "Fiber optical parametric amplifiers with circularly-polarized pumps," Electron. Lett. **39**, 350–351 (2003).
13. R. W. Boyd, *Nonlinear Optics*, 2nd ed. (Academic, San Diego, Calif. 2003).
14. J. P. Gordon and H. Kogelnik, "PMD fundamentals: polarization mode dispersion in optical fibers," Proc. Natl. Acad. Sci. U.S.A. **97**, 4541–4550 (2000).
15. L. Mandel and E. Wolf, *Optical Coherence and Quantum Optics* (Cambridge U. Press, New York, 1995), Chap. 10.
16. S. Huard, *Polarization of Light* (Wiley, New York, 1997).
17. A. V. Mikhailov and S. Wabnitz, "Polarization dynamics of counterpropagating beams in optical fibers," Opt. Lett. **15**, 1055–1057 (1990).
18. S. Wabnitz and B. Daino, "Polarization domains and instabilities in nonlinear optical fibers," Phys. Rev. A **182**, 289–293 (1993).
19. Q. Lin and G. P. Agrawal, "Effects of polarization-mode dispersion on fiber-based parametric amplification and wavelength conversion," Opt. Lett. **29**, 1114–1116 (2004).
20. F. Yaman, Q. Lin, and G. P. Agrawal, "Effects of polarization-mode dispersion in dual-pump fiber-optic parametric amplifiers," IEEE Photon. Technol. Lett. **16**, 431–433 (2004).